Optics Communications 366 (2016) 8–12

Contents lists available at ScienceDirect

Optics Communications

journal homepage: www.elsevier.com/locate/optcom

Invited Paper

Improving the signal-to-noise ratio of thermal ghost imaging based on positive–negative intensity correlation

Shu-Chun Song [a], Ming-Jie Sun [a,*], Ling-An Wu [b]

[a] School of Instrument Science and Optoelectronics Engineering, Beihang University, Beijing 100191, China
[b] Laboratory of Optical Physics, Institute of Physics and Beijing National Laboratory for Condensed Matter Physics, Chinese Academy of Sciences, Beijing 100190, China

ARTICLE INFO

Article history:
Received 31 October 2015
Received in revised form
17 December 2015
Accepted 17 December 2015
Available online 23 December 2015

Keywords:
Ghost imaging
Positive-negative intensity correlation
Signal-to-noise ratio
Intensity fluctuation

ABSTRACT

Ghost imaging with thermal light is a topic in optical imaging that has aroused great interest in recent years. However, the imaging quality must be greatly improved before the technology can be transferred from the lab to engineering applications. By means of correspondence ghost imaging (CGI) with a pseudo-thermal light source and appropriate sorting of the intensity fluctuations of the signal and reference beams, we obtain the positive and negative Hanbury Brown and Twiss intensity correlation characteristics of the optical field. Then, for ghost imaging of a transmissive binary object, we find that by subtracting the negative from the positive fluctuation frames of the presorted reference detector signals, the signal-to-noise ratio can be effectively increased, with almost all the background noise eliminated. Our results show that, compared with the generic CGI technique, the signal-to-noise ratio can be increased by nearly 60%.

1. Introduction

In a "ghost" imaging system, light is divided into two spatially correlated beams, one beam passes through the object and illuminates a "bucket" detector which has no spatial resolution and only collects the total intensity, while the other does not interact with the object and its intensity is measured by a pixelated "reference" detector. Surprisingly, the image of the object can be retrieved by the correlation measurement of the intensities at the two detectors. The principle behind this comes from the intensity interference experiment that Hanbury Brown and Twiss [1] performed to measure the angular size of distant stars in 1956.

The first ghost image [2] was obtained with entangled photon pairs generated by spontaneous parametric down-conversion, so it was once considered to be a phenomenon peculiar to quantum optics. Later, it was shown theoretically and experimentally that ghost imaging (GI) could be realized with a classical thermal light source [3–6]. Compared with standard imaging modalities, GI has been shown to have potential for enhanced resolution and visibility in harsh environments [7–11]. However, the visibility of the images reconstructed from thermal light is low (defined as $(I_{max}-I_{min})/(I_{max}+I_{min})$), therefore various methods [12–17] have been devised to improve this, such as high-order GI [13–16], and increasing the intensity fluctuations of thermal light [17]. A scheme called differential GI [18] can greatly enhance the signal-to-noise ratio (SNR) of traditional GI. Recently, a technique called correspondence ghost imaging (CGI) [19] was proposed by Luo et al., in which a positive and negative image is reconstructed only by conditional averaging of the reference detector intensities, no longer requiring conventional correlation calculation, so the computation time is greatly reduced while the image visibility and SNR are increased.

In this paper, the intensities of the signal and reference beams are sorted according to their values relative to their respective mean values. In this way, we can measure the positive–positive, positive–negative, negative–positive, and negative–negative correspondence intensities of the two beams. By combining the positive with the inverted negative intensity values, the GI quality is considerably improved; the SNR of the retrieved images is taken as the measure of quality, and analyzed.

2. Experimental scheme

The basic experimental setup for GI is shown in Fig. 1. Pseudo-thermal light, generated by a linearly polarized He-Ne laser beam illuminating a ground-glass plate rotating at a speed of 3 rad/min, is separated by a beam splitter (BS) into two correlated arms. In the signal arm, the light passes through an object and the total intensity I_2 is collected by the bucket detector D2, while in the

* Corresponding author.
E-mail address: Mingjie.Sun@buaa.edu.cn (M.-J. Sun).

http://dx.doi.org/10.1016/j.optcom.2015.12.045
0030-4018/

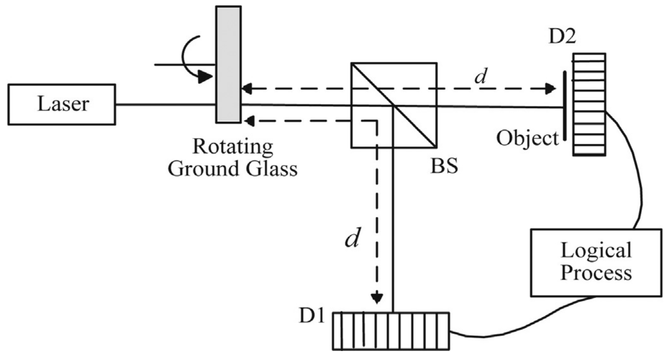

Fig. 1. Schematic of thermal ghost imaging. BS: beamsplitter, D1: reference detector, D2: bucket detector.

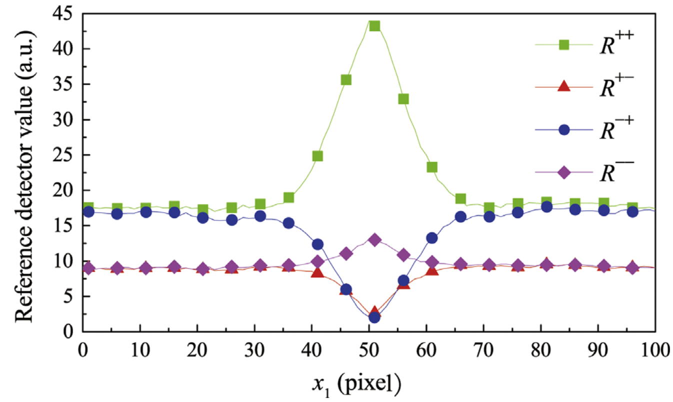

Fig. 2. HBT intensity correlation of the pseudo-thermal light source, R^{++}: positive–positive, R^{+-}: positive–negative, R^{-+}: negative–positive, and R^{--}: negative–negative.

reference arm, the light goes directly to detector D1, which records the intensity distribution $I_1(x_1)$, where x_1 is the transverse spatial coordinate. Actually, both D1 and D2 are charge-coupled device (CCD) cameras (Imaging Source DMK 31BU03), but D2 is used as a bucket detector to calculate the total light intensity through the object. In order to ensure that the pseudo-thermal field distribution at the reference detector is identical to that at the object plane, the distance from the source to the object must be the same as that to detector D1 (CCD), that is, d=230 mm. Both detectors are triggered synchronously by the same signal generator at a rate of 22 Hz.

First, it is necessary to understand the statistical characteristics of our pseudo-thermal light source, so we measured its HBT intensity correlation without any object. The readouts from detectors D2 and D1 were directly processed according to the CGI method, as described below.

The intensity $I_2(t_i)$ at D2 based on the calculated average intensity $\langle I_2\rangle$can be divided into positive and negative fluctuations, the former satisfying $I_2(t_i) \geq \langle I_2\rangle$ and the latter $I_2(t_i) < \langle I_2\rangle$. Correspondingly, because both detectors are synchronized in time, the reference signals $I_1(x_1, t_i)$may also be separated into two subsets according to the sign of the fluctuations of $I_2(t_i)$:

$$I_1^+(x_1, t_i) = \{t_i | I_2(t_i) \geq \langle I_2\rangle\}$$
$$I_1^-(x_1, t_i) = \{t_i | I_2(t_i) < \langle I_2\rangle\}, \tag{1}$$

where $\langle ... \rangle$ represents the ensemble average and t_i denotes the measurement time. If we now examine the intensities of the reference beam within each subset, we find that they also show positive and negative fluctuations relative to the total ensemble average $\langle I_1\rangle$ of the reference detector measurements, averaged over both spatial coordinates and time. That is, after $\langle I_1\rangle$ has been determined, the groups $I_1^+(x_1, t_i)$ and $I_1^-(x_1, t_i)$ can be further separated into the following positive and negative parts:

$$I_1^{++}(x_1, t_i) = \{t_i | I_2(t_i) \geq \langle I_2\rangle, I_1(x_1, t_i) \geq \langle I_1\rangle\},$$
$$I_1^{+-}(x_1, t_i) = \{t_i | I_2(t_i) \geq \langle I_2\rangle, I_1(x_1, t_i) < \langle I_1\rangle\},$$
$$I_1^{-+}(x_1, t_i) = \{t_i | I_2(t_i) < \langle I_2\rangle, I_1(x_1, t_i) \geq \langle I_1\rangle\},$$
$$I_1^{--}(x_1, t_i) = \{t_i | I_2(t_i) < \langle I_2\rangle, I_1(x_1, t_i) < \langle I_1\rangle\}. \tag{2}$$

The corresponding positive–positive, positive–negative, negative–positive, negative–negative intensity average values can then be calculated as:

$$R^{++}(x_1) = \frac{1}{N_+}\sum I_1^{++}(x_1, t_i), \quad R^{+-}(x_1) = \frac{1}{N_+}\sum I_1^{+-}(x_1, t_i),$$
$$R^{-+}(x_1) = \frac{1}{N_-}\sum I_1^{-+}(x_1, t_i), \quad R^{--}(x_1) = \frac{1}{N_-}\sum I_1^{--}(x_1, t_i), \tag{3}$$

where N_+ and N_- are the total number of frames for $I_2(t_i) \geq \langle I_2\rangle$ and $I_2(t_i) < \langle I_2\rangle$, respectively.

In the experiment, a total of 20,000 frames were taken by each camera. The HBT intensity correlation values as a function of the CCD camera pixel position are plotted in Fig. 2, where the curves are all calculated from experimentally measured data, but if all the points were plotted they would be too dense so only certain points are shown, with the squares, triangles, dots and diamonds denoting the values of R^{++},R^{+-}, R^{-+}, and R^{--}, respectively. Each point was calculated after averaging the values of each pixel of the CCD camera. From the figure, we can see that the $(+,+)$ and $(-,-)$ plots are similar to the HBT positive correlation curves of thermal light, while the $(+,-)$and $(-,+)$ plots demonstrate a negative correlation feature. When we use the positive fluctuations of the bucket detector as an indicator for the reference beam, we can observe both positive (R^{++}) and negative (R^{+-}) correlation features, while the generic CGI technique only produces a positive correlation R^+_{CGI}. We may now redefine a positive correspondence intensity correlation R^+ within the $I_2(t_i) \geq \langle I_2\rangle$ condition as a positive–positive intensity R^{++} minus a positive–negative intensity R^{+-}:

$$R^+ = R^{++} - R^{+-}. \tag{4}$$

Similarly, using the negative fluctuations of the bucket detector as the indicator, the negative reference detector fluctuations R^- can be retrieved as:

$$R^- = R^{-+} - R^{--}. \tag{5}$$

The normalized positive values of R^+ and R^+_{CGI} are shown in Fig. 3(a), where it is clear that the background noise of R^+ (blue solid line) is significantly lower than that of R^+_{CGI} (red dash line). A similar comparison for the normalized negative fluctuations is shown in Fig. 3(b), where again we see that the background noise of R^- is significantly suppressed compared with R^-_{CGI}. Interestingly, by introducing the normalization algorithm, the visibility of the intensity correlation always reaches 1 according to its definition, regardless of the noise. Therefore the SNR may be employed more precisely to compare the quality of images.